Widely-Linear Multi-Branch Decision Feedback Detection Algorithms for Large-Scale Multiple-Antenna Systems

Rodrigo C. de Lamare
CETUC, Pontifical Catholic University of Rio de Janeiro, Brazil
Department of Electronics, University of York, York Y010 5DD, United Kingdom
Emails: delamare@cetuc.puc-rio.br, rcdl500@york.ac.uk

***Abstract*—This paper presents widely-linear multi-branch decision feedback detection techniques for large-scale multiuser multiple-antenna systems. We consider a scenario with impairments in the radio-frequency chain in which the in-phase (I) and quadrature (Q) components exhibit an imbalance, which degrades the receiver performance and originates non-circular signals. A widely-linear multi-branch decision feedback receiver is developed to mitigate both the multiuser interference and the I/Q imbalance effects. An iterative detection and decoding scheme with the proposed receiver and convolutional codes is also devised. Simulation results show that the proposed techniques outperform existing algorithms.**

***Keywords*—Massive MIMO, widely-linear processing, decision-feedback receivers, iterative detection and decoding techniques.**

I. Introduction

Large-scale multiple-antenna systems have recently attracted substantial interest due to their potential for deployment in the next generation of wireless networks. In particular, large-scale multiple-antenna systems have the ability to offer a substantial increase in data rates and to mitigate interference more effectively due to the extra degrees of freedom offered by the large number of antennas [1], [2]. Despite the several advantages of large-scale multiple-antenna systems, there are many problems that need to be solved before such systems could be adopted in practice. Among them are the development of efficient detectors that can obtain high performance with reduced cost and operate in the presence of hardware impairments [2].

In the literature, the use of the receive matched filter (RMF) is often advocated when the number of antennas is substantially increased and the channels become asymptotically orthogonal [2], [3]. Furthermore, these studies assume knowledge of the channels and seldom include hardware impairments [4]. However, in the presence of non-orthogonal channels the access point or the users will be affected by multiuser interference, which requires more sophisticated detection algorithms than the receive matched filter [5], [6], [7]. Linear detectors [8], successive interference cancellation (SIC) [10], [12], likelihood-ascent search (LAS) techniques [9], [10] decision feedback (DF) [13], [14], [15] and their variants are techniques that have attractive trade-offs between performance and complexity.

With the increase of the number of antennas and associated radio frequency (RF) chains, the size and cost-effectiveness of individual RF chains eventually becomes critical [16]. A technical solution to such large-scale systems is the direct-conversion radio (DCR) architecture, which is flexible and can operate with different air interfaces, frequency bands and waveforms. Conversely, it does not require RF image rejection filters nor intermediate frequency stages, resulting in lower implementation cost and smaller sizes than the classic super-heterodyne structure. A limitation of DCR is a common RF imperfection known as in-phase quadrature (I/Q) imbalance, which appears due to non-ideal properties of RF mixers and leads to performance degradation.

978-1-4673-6540-6/15/$31.00

The I/Q imbalance may also originate non-circular signals even in the presence of circular source signals, which can be exploited by widely-linear signal processing techniques [17]-[20]. Prior work on widely-linear processing for wireless receivers includes several studies on multiple-antenna receivers [17], [18], single-antenna interference cancellation concepts [19], and large-scale multiple antenna systems [20].

In this work, we investigate a potential solution to large-scale multiple-antenna systems that suffer from I/Q imbalance and exhibit non-orthogonal channels. In particular, we combine widely-linear processing techniques and the multi-branch concept [13], [15] in order to devise a widely-linear multi-branch decision feedback (WL-MB-DF) receiver that can mitigate I/Q imbalance and achieve a near-optimal performance. An iterative detection and decoding scheme with the proposed receiver and convolutional codes is also devised. Simulation results show that the proposed algorithms outperform prior art.

The remainder of this work is structured as follows. Section II describes the uplink of a multiuser multiple-antenna system, models the I/Q imbalance and characterizes the second-order statistics of the received data. Section III presents the proposed WL-MB-DF receiver. An iterative detection and decoding scheme based on the WL-MB-DF is developed in Section IV. Section V illustrates and discusses the simulation results, whereas Section VI gives the conclusions.

II. System model and statistical modelling of I/Q imbalance

In this section, we detail the uplink of a multiuser multiple-antenna system, model the I/Q imbalance and characterize the second-order statistics of the received data.

A. Uplink system model

We consider the uplink of a multiuser massive multiple-antenna system where the base station employs N_A antenna elements at the receiver. The scenario of interest includes K users which are equipped with N_U antenna elements and communicate with a receiver with N_A antenna elements, where $N_A \geq KN_U$. At each time instant, the K users transmit N_U symbols which are organized into a $N_U \times 1$ vector $\boldsymbol{s}_k[i] = \left[s_{k,1}[i],\ s_{k,2}[i],\ \ldots,\ s_{k,N_U}[i]\right]^T$ taken from a modulation constellation $A = \{a_1,\ a_2,\ \ldots,\ a_N\}$. The data symbols of each user are organized in $N_U \times 1$ vectors $\boldsymbol{s}_k[i]$ and transmitted over flat fading channels. The received signal after

demodulation, pulse matched filtering and sampling is collected in an $N_A \times 1$ vector $\boldsymbol{r}[i] = \left[r_1[i],\ r_2[i],\ \ldots,\ r_{N_R}[i]\right]^T$ with sufficient statistics for processing as described by

$$\boldsymbol{r}[i] = \sum_{k=1}^{K} \boldsymbol{H}_k \boldsymbol{s}_k[i] + \boldsymbol{n}[i], \tag{1}$$

where the $N_A \times 1$ vector $\boldsymbol{n}[i]$ is a zero mean complex circular symmetric Gaussian noise vector with covariance matrix $E\left[\boldsymbol{n}[i]\boldsymbol{n}^H[i]\right] = \sigma_n^2 \boldsymbol{I}$. The data vectors $\boldsymbol{s}_k[i]$ have zero mean and covariance matrices $\boldsymbol{Q}_k = E\left[\boldsymbol{s}_k[i]\boldsymbol{s}_k^H[i]\right] = \sigma_{s_k}^2 \boldsymbol{I}$, where $\sigma_{s_k}^2$ is the signal power. The elements h_{n_A,n_U} of the $N_A \times N_U$ channel matrices $\boldsymbol{H}_k$ represent the complex channel gains from the n_Uth transmit antenna to the n_Ath receive antenna.

B. Modelling and characterization of I/Q imbalance

DCR converts the received RF signal to two real-valued baseband signals, denoted I and Q components, respectively. The conversion is often performed with two local oscillator signals and mixers, which have equal gains and 90 degrees phase difference. However, in practice signals and mixers have a gain mismatch and they are not in perfect phase quadrature. For this reason, the statistics of the received signal change and the corresponding complex signal, even if originally circular, becomes non-circular. This effect is called I/Q imbalance [16]. The received signal with I/Q imbalance is described by

$$\begin{aligned} \boldsymbol{r}_{\mathrm{IQ}}[i] &= \boldsymbol{A}_1 \boldsymbol{r}[i] + \boldsymbol{A}_2 \boldsymbol{r}^*[i] \\ &= \sum_{k=1}^{K} \boldsymbol{A}_1 \boldsymbol{H}_k \boldsymbol{s}_k[i] + \sum_{k=1}^{K} \boldsymbol{A}_2 \boldsymbol{H}_k^* \boldsymbol{s}_k^*[i] \\ &\quad + \boldsymbol{A}_1 \boldsymbol{n}[i] + \boldsymbol{A}_2 \boldsymbol{n}^*[i], \end{aligned} \tag{2}$$

where the $N_A \times N_A$ diagonal matrices $\boldsymbol{A}_j = \mathrm{diag}\left(A_{j,1}\ A_{j,2} \ldots A_{j,N_A}\right)$ for $j = 1, 2$ contain the I/Q imbalance components with entries given by

$$A_{1,i} = (1+g_i e^{-j\phi_i}), \quad A_{2,i} = (1-g_i e^{-j\phi_i})/2, \ \ i = 1, \ldots, N_A \tag{3}$$

where g_i represents the relative gain mismatch and for the ith antenna element and ϕ_i corresponds to the phase mismatch between the I- and Q-branches. Note that in the absence of I/Q imbalance we have $g_i = 1$ and $\phi_i = 0$.

In order to characterize the I/Q imbalance, let us consider the covariance and pseudo-covariance matrices of the data. The covariance matrix of $\boldsymbol{r}[i]$ in (1) is given by

$$\boldsymbol{R} \triangleq E[\boldsymbol{r}[i]\boldsymbol{r}^H[i]] = \sum_{k=1}^{K} \boldsymbol{H}_k \boldsymbol{Q}_k \boldsymbol{H}_k^H + \sigma_n^2 \boldsymbol{I}, \tag{4}$$

and the pseudo-covariance matrix of $\boldsymbol{r}[i]$ is defined by

$$\boldsymbol{C} \triangleq E[\boldsymbol{r}[i]\boldsymbol{r}^T[i]] = \sum_{k=1}^{K} \boldsymbol{H}_k \boldsymbol{P}_k \boldsymbol{H}_k^T, \tag{5}$$

where the $N_U \times N_U$ pseudo-covariance matrix is given by $\boldsymbol{P}_k = E[\boldsymbol{s}_k \boldsymbol{s}_k^T] = \begin{cases} \sigma_{s_k}^2 \boldsymbol{I} & \text{for BPSK, ASK, etc,} \\ 0 & \text{for QPSK, QAM, etc.} \end{cases}$

In order to model and statistically characterize the non-circular received signal in (2), we rely on the second-order statistics of the augmented data, which yields the augmented received signal described by

$$\boldsymbol{r}_a[i] \triangleq \begin{bmatrix} \boldsymbol{r}_{\mathrm{IQ}}[i] \\ \boldsymbol{r}_{\mathrm{IQ}}^*[i] \end{bmatrix}, \tag{6}$$

and the covariance matrix of $\boldsymbol{r}_a[i]$ is given by

$$\boldsymbol{R}_a[i] \triangleq E[\boldsymbol{r}_a[i]\boldsymbol{r}_a^H[i]] = \begin{bmatrix} \boldsymbol{R}_{\mathrm{IQ}} & \boldsymbol{C}_{\mathrm{IQ}} \\ \boldsymbol{C}_{\mathrm{IQ}}^* & \boldsymbol{R}_{\mathrm{IQ}}^* \end{bmatrix}, \tag{7}$$

where for arbitrary gain and phase mismatches ($g_i \neq 1$ and $\phi_i \neq 0$) the covariance matrix of $\boldsymbol{r}_{\mathrm{IQ}}[i]$ is described by $\boldsymbol{R}_{\mathrm{IQ}} \triangleq \boldsymbol{A}_1 \boldsymbol{R} \boldsymbol{A}_1^H + \boldsymbol{A}_1 \boldsymbol{C} \boldsymbol{A}_2^H + \boldsymbol{A}_2 \boldsymbol{C}^* \boldsymbol{A}_1^H + \boldsymbol{A}_2 \boldsymbol{R}^* \boldsymbol{A}_2^H$ and the pseudo-covariance of $\boldsymbol{r}_{\mathrm{IQ}}[i]$ is $\boldsymbol{C}_{\mathrm{IQ}} \triangleq \boldsymbol{A}_1 \boldsymbol{C} \boldsymbol{A}_1^T + \boldsymbol{A}_1 \boldsymbol{R} \boldsymbol{A}_2^T + \boldsymbol{A}_2 \boldsymbol{R}^* \boldsymbol{A}_1^T + \boldsymbol{A}_2 \boldsymbol{C}^T \boldsymbol{A}_2^T$.

Several other cases of interest relating the gain and phase mismatches and the pseudo-covariance matrix $\boldsymbol{C}$ can be used to characterize $\boldsymbol{R}_{\mathrm{IQ}}$ and $\boldsymbol{C}_{\mathrm{IQ}}$, namely:

- When $\boldsymbol{C} = \boldsymbol{0}$, $g_i = 1$ and $\phi_i = 0$, we have $\boldsymbol{A}_1 = \boldsymbol{I}$, $\boldsymbol{A}_2 = \boldsymbol{0}$, $\boldsymbol{R}_{\mathrm{IQ}} = \boldsymbol{R}$ and $\boldsymbol{C}_{\mathrm{IQ}} = \boldsymbol{0}$.
- When $\boldsymbol{C} = \boldsymbol{0}$, $g_i \neq 1$ and $\phi_i \neq 0$, we have $\boldsymbol{A}_1 \neq \boldsymbol{I}$, $\boldsymbol{A}_2 \neq \boldsymbol{0}$, $\boldsymbol{R}_{\mathrm{IQ}} = \boldsymbol{A}_1 \boldsymbol{R} \boldsymbol{A}_2^H$ and $\boldsymbol{C}_{\mathrm{IQ}} = \boldsymbol{A}_1 \boldsymbol{R} \boldsymbol{A}_2^T + \boldsymbol{A}_2 \boldsymbol{R}^* \boldsymbol{A}_1^T$.
- When $\boldsymbol{C} \neq \boldsymbol{0}$, $g_i = 1$ and $\phi_i = 0$, we have $\boldsymbol{A}_1 = \boldsymbol{I}$, $\boldsymbol{A}_2 = \boldsymbol{0}$, $\boldsymbol{R}_{\mathrm{IQ}} = \boldsymbol{R}$ $\boldsymbol{C}_{\mathrm{IQ}} = \boldsymbol{C}$.

Note that even for $\boldsymbol{C} = \boldsymbol{0}$ due to circular transmitted data, the I/Q imbalance can result in non circular data $\boldsymbol{C}_{\mathrm{IQ}} \neq \boldsymbol{0}$, which can be exploited by widely-linear processing techniques.

III. Proposed Widely-Linear Decision Feedback Detection

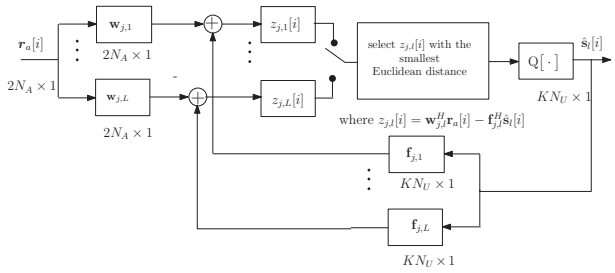

Fig. 1. Block diagram of the proposed WL-MB-DF detector and the processing of the jth data stream.

In this section, the structure of the proposed WL-MB-DF detector is presented and a schematic of the detector is shown in Fig. 1. The WL-MB-DF detector employs multiple pairs of widely-linear minimum-mean square error (WL-MMSE) receive filters in such a way that the detector can obtain different local maxima of the likelihood function and select the best candidate for detection according to the Euclidean distance for each received data symbol. The WL-MB-DF scheme is flexible and approaches the full receive diversity available in the system by increasing the number of branches.

In order to detect each transmitted data stream using the WL-MB-DF detector, the receiver linearly combines the feedforward filter represented by the $2N_A \times 1$ vector $\boldsymbol{w}_{j,l}$ corresponding to the j-th data stream and the l-th branch with $\boldsymbol{r}_a[i]$, subtracts the remaining interference by linearly

combining the feedback filter denoted by the $KN_U \times 1$ vector $\boldsymbol{f}_{j,l}$ with the $KN_U \times 1$ vector of initial decisions $\hat{\boldsymbol{s}}_l[i]$ obtained by $\boldsymbol{w}_{j,l}$. This process is repeated for L candidate symbols and KN_U data streams as described by

$$\begin{aligned} z_{j,l}[i] &= \boldsymbol{w}_{j,l}^H \boldsymbol{r}_a[i] - \boldsymbol{f}_{j,l}^H \hat{\boldsymbol{s}}_l[i], \\ & j = 1, \ \ldots, \ KN_U \ \text{ and } \ l = 1, \ \ldots, \ L, \end{aligned} \tag{8}$$

where the input to the decision device for the ith symbol and the j-th stream is the $L \times 1$ vector $\boldsymbol{z}_j[i] = [z_{j,1}[i] \ \ldots \ z_{j,L}[i]]^T$.

The WL-MB-DF detector generates L candidate symbols for each data stream and then selects the best branch according to the Euclidean distance as described by

$$\begin{aligned} l_{j,\text{opt}} &= \arg \min_{1 \le l_j \le L} \mathrm{C}(\boldsymbol{r}_a[i], \boldsymbol{H}, \hat{\boldsymbol{s}}_l[i], \boldsymbol{w}_{j,l}, \boldsymbol{f}_{j,l}), \\ & j = 1, \ \ldots, \ KN_U, \end{aligned} \tag{9}$$

where

$$\mathrm{C}(\boldsymbol{r}_a[i], \boldsymbol{H}, \hat{\boldsymbol{s}}_l[i], \boldsymbol{w}_{j,l}, \boldsymbol{f}_{j,l})) = ||\boldsymbol{r}_a[i] - \boldsymbol{H}\hat{\boldsymbol{s}}_l[i]|| \tag{10}$$

is the Euclidean distance between $\boldsymbol{r}_a[i]$ and the product of the channels of all users $\boldsymbol{H} = [\boldsymbol{H}_1 \ldots \boldsymbol{H}_k]$ and the candidate symbol vector $\hat{\boldsymbol{s}}_l[i]$. The final detected symbol of the WL-MB-DF detector is obtained by using the best branch:

$$\begin{aligned} \hat{s}_j[i] &= Q\big[\boldsymbol{z}_{j,l_{j,\text{opt}}}[i]\big] = Q\big[\boldsymbol{w}_{j,l_{j,\text{opt}}}^H \boldsymbol{r}_a[i] - \boldsymbol{f}_{j,l_{j,\text{opt}}}^H \hat{\boldsymbol{s}}_{l_{j,\text{opt}}}[i]\big], \\ & j = 1, \ \ldots, \ KN_U, \end{aligned} \tag{11}$$

where $Q(\cdot)$ is a function that decides about the symbols, which can be drawn from an M-PSK or a QAM constellation.

A. WL-MMSE Filter Design

The design of the receive filters is equivalent to determining $\boldsymbol{w}_{j,l}$ and $\boldsymbol{f}_{j,l}$ subject to certain shape constraints on $\boldsymbol{f}_{j,l}$ in accordance to the following optimization problem

$$\begin{aligned} &\min \ \mathrm{MSE}(s_j[i], \boldsymbol{w}_{j,l}, \boldsymbol{f}_{j,l}) = E\big[|s_j[i] - \boldsymbol{w}_{j,l}^H \boldsymbol{r}_a[i] + \boldsymbol{f}_{j,l}^H \hat{\boldsymbol{s}}_l[i]|^2\big] \\ &\quad \text{subject to } \boldsymbol{S}_{j,l}\boldsymbol{f}_{j,l} = \boldsymbol{0} \ \text{ and } \ ||\boldsymbol{f}_{j,l}||^2 = \gamma_{j,l}||\boldsymbol{f}_{j,l}^c||^2, \\ &\text{for } j = 1, \ldots, KN_U \text{ and } l = 1, \ldots, L, \end{aligned} \tag{12}$$

where the $KN_U \times KN_U$ shape constraint matrix is $\boldsymbol{S}_{j,l}$, $\boldsymbol{0}$ is a $KN_U \times 1$ constraint vector and $\gamma_{j,l}$ is a design parameter that ranges from 0 to 1 and is responsible for scaling the norm of the conventional feedback receive filter $\boldsymbol{f}_{j,l}^c$. The scaling of $\boldsymbol{f}_{j,l}^c$ results in the desired feedback receive filter $\boldsymbol{f}_{j,l}$.

In what follows, WL-MMSE receive filters based on the proposed optimization in (12) are derived. By resorting to the method of Lagrange multipliers, computing the gradient vectors of the Lagrangian with respect to $\boldsymbol{w}_{j,l}$ and $\boldsymbol{f}_{j,l}$, equating them to null vectors and rearranging the terms, we obtain for $j = 1, \ldots, KN_U$ and $l = 1, \ldots, L$

$$\boldsymbol{w}_{j,l}^{\text{MMSE}} = \boldsymbol{R}_a^{-1}(\boldsymbol{p}_{a,j} + \boldsymbol{Q}_a \boldsymbol{f}_{j,l}), \tag{13}$$

$$\boldsymbol{f}_{j,l}^{\text{MMSE}} = \frac{\beta_{j,l}}{\sigma_s^2} \boldsymbol{\Pi}_{j,l} \boldsymbol{Q}_a^H \boldsymbol{w}_{j,l}, \tag{14}$$

where the $2N_A \times 1$ augmented cross-correlation vector is

$$\boldsymbol{p}_{a,j} \triangleq E[\boldsymbol{r}_a[i] s_j^*[i]] = \begin{pmatrix} \boldsymbol{A}_1 \boldsymbol{H}_j \boldsymbol{q}_j + \boldsymbol{A}_2 \boldsymbol{H}_j^* \boldsymbol{p}_j \\ \boldsymbol{A}_1^* \boldsymbol{H}_j^* \boldsymbol{p}_j + \boldsymbol{A}_2^* \boldsymbol{H}_j \boldsymbol{q}_j \end{pmatrix}, \tag{15}$$

where $\boldsymbol{q}_j = E[\boldsymbol{s}_k[i] s_j^*[i]] = \sigma_{s_k}^2 \boldsymbol{t}_j$, $\boldsymbol{t}_j$ is an $N_U \times 1$ vector with a one in the jth entry and zeros elsewhere, the $N_U \times 1$ cross-correlation vector is

$$\boldsymbol{p}_j = E[\boldsymbol{s}_k^*[i] s_j^*] = \begin{cases} \sigma_{s_k}^2 \boldsymbol{t}_j & \text{for BPSK, ASK, etc,} \\ \boldsymbol{0} \ (\boldsymbol{C} = \boldsymbol{0}) & \text{for QPSK, QAM, etc} \end{cases}$$

and the $2N_A \times KN_U$ cross-correlation matrix is given by

$$\boldsymbol{Q}_a \triangleq E\big[\boldsymbol{r}_a[i] \hat{\boldsymbol{s}}_l^H[i]\big] = \begin{pmatrix} \sigma_{s_k}^2 \boldsymbol{A}_1 \boldsymbol{H} + \sigma_{s_k}^2 \boldsymbol{A}_2 \boldsymbol{H}^* \\ \sigma_{s_k}^2 \boldsymbol{A}_1^* \boldsymbol{H}_j^* + \sigma_{s_k}^2 \boldsymbol{A}_2^* \boldsymbol{H} \end{pmatrix}, \tag{16}$$

where

$$\boldsymbol{\Pi}_{j,l} = \boldsymbol{I} - \boldsymbol{S}_{j,l}^H (\boldsymbol{S}_{j,l}^H \boldsymbol{S}_{j,l})^{-1} \boldsymbol{S}_{j,l} \tag{17}$$

is a projection matrix that ensures the shape constraint $\boldsymbol{S}_{j,l}$ on the feedback filter, $\beta_{j,l} = (1 - \mu_{j,l})^{-1}$ is the parameter that controls the ability of the WL-MB-DF detector to mitigate error propagation with values $0 \le \beta_{j,l} \le 1$, and $\mu_{j,l}$ is the Lagrange multiplier. Note that the inverse $(\boldsymbol{S}_{j,l}^H \boldsymbol{S}_{j,l})^{-1}$ might not exist. In these situations, a pseudo-inverse is computed. The relationship between $\beta_{j,l}$ and $\gamma_{j,l}$ is not in closed-form except for the extreme values when we have $\beta_{j,l} = 0$ and $\beta_{j,l} = 1$ for $\gamma_{j,l} = 0$ (standard WL MMSE detector) and $\gamma_{j,l} = 1$ (standard WL-MB-DF detector), respectively. The above expressions only depend on statistical quantities, and consequently on the channel matrix $\boldsymbol{H}$, the symbol and noise variances $\sigma_{s_j}^2$ and σ_n^2, respectively, and the constraints.

The MMSE associated with the filters $\boldsymbol{w}_{j,l}^{\text{MMSE}}$ and $\boldsymbol{f}_{j,l}^{\text{MMSE}}$ and the statistics of the data symbols $s_j[i]$ is given by

$$\begin{aligned} \underbrace{\mathrm{MSE}(s_j[i], \boldsymbol{w}_{j,l}^{\text{MMSE}}, \boldsymbol{f}_{j,l}^{\text{MMSE}})}_{\mathrm{MMSE}_j} &= \sigma_{s_j}^2 - \boldsymbol{w}_{j,l}^{H,\ \text{MMSE}} \boldsymbol{R}_a \boldsymbol{w}_{j,l}^{\text{MMSE}} \\ &\quad + \boldsymbol{f}_{j,l}^{H,\ \text{MMSE}} \boldsymbol{f}_{j,l}^{\text{MMSE}}, \end{aligned} \tag{18}$$

where $\sigma_{s_j}^2 = E[|s_j[i]|^2]$ is the variance of the desired symbol.

B. Design of Shape Constraint Matrices and Ordering

The shape constraint matrices $\boldsymbol{S}_{j,l}$ modify the structure of the feedback filters $\boldsymbol{f}_{j,l}$ in such a way that only the selected feedback elements of $\boldsymbol{f}_{j,l}$ will be used to cancel the interference between the data streams. The feedback connections perform interference cancellation with a chosen ordering. For the first branch of detection ($l = 1$), we employ

$$\begin{aligned} &\boldsymbol{S}_{j,l}\boldsymbol{f}_{j,l} = \boldsymbol{0}, \quad l = 1, \ j = 1, \ldots, KN_U, \\ &\boldsymbol{S}_{j,l} = \begin{bmatrix} \boldsymbol{0}_{KN_U - j + 1, KN_U - j + 1} & \boldsymbol{0}_{KN_U - j + 1, j - 1} \\ \boldsymbol{0}_{j-1, KN_U - j + 1} & \boldsymbol{I}_{j-1, j-1} \end{bmatrix}, \end{aligned} \tag{19}$$

where $\boldsymbol{0}_{m,n}$ denotes an $m \times n$-dimensional matrix full of zeros, and $\boldsymbol{I}_m$ denotes an m-dimensional identity matrix. For the remaining branches, an approach based on permutations in the matrices $\boldsymbol{S}_{j,l}$ is adopted, which is given by

$$\begin{aligned} &\boldsymbol{S}_{j,l}\boldsymbol{f}_{j,l} = \boldsymbol{0}, \quad l = 2, \ldots, L, \ j = 1, \ldots, KN_U, \\ &\boldsymbol{S}_{j,l} = \phi_l \begin{bmatrix} \boldsymbol{0}_{KN_U - j + 1, KN_U - j + 1} & \boldsymbol{0}_{KN_U - j + 1, j - 1} \\ \boldsymbol{0}_{j-1, KN_U - j + 1} & \boldsymbol{I}_{j-1, j-1} \end{bmatrix}, \end{aligned} \tag{20}$$

where the operator $\phi_l[\cdot]$ permutes the elements of the argument matrix such that this results in different cancellation patterns.

For the first branch, an ordering algorithm based on increasing values of the MMSE is considered. The ordering of the remaining branches depends on the maximization of the difference between the MMSE of different data streams:

$$o_{j,l} = \arg\max_{n} \sum_{q=1}^{j-1} |\text{MMSE}_n - \text{MMSE}_{o_{j,q}}|,$$
$$\text{for } l = 2, \ \ldots, \ L \text{ and } j, n = 1, \ldots, KN_U$$
$$\text{subject to } \ \text{MMSE}_{o_{j,l}} \neq \text{MMSE}_{o_{q,l}}, \ q = 1, \ldots, j-1. \tag{21}$$

IV. Iterative Processing

This section presents an iterative version of the proposed WL-MB-DF detector operating with soft-input soft-output detection and decoding, and with convolutional codes [11]-[21]. The receiver structure consists of the following stages: a soft-input-soft-output (SISO) WL-MB-DF detector and a maximum *a posteriori* (MAP) decoder. These stages are separated by interleavers and deinterleavers. The soft outputs from the WL-MB-DF are used to estimate log-likelihood ratios (LLRs) which are interleaved and serve as input to the MAP decoder for the convolutional code. The MAP decoder computes *a posteriori* probabilities (APPs) for each stream's encoded symbols, which are used to generate soft estimates. These soft estimates are used to update the receive filters of the WL-MB-DF detector, de-interleaved and fed back through the feedback filter. The WL-MB-DF detector computes the *a posteriori* log-likelihood ratio (LLR) of a transmitted symbol ($+1$ or -1) for every code bit of each stream as given by

$$\begin{aligned}\Lambda_1[b_{j,c,l}[i]] &= \log\frac{P[\boldsymbol{r}_a[i]|b_{j,c,l}[i]=+1]}{P[\boldsymbol{r}_a[i]|b_{j,c,l}[i]=-1]} + \log\frac{P[b_{j,c}[i]=+1]}{P[b_{j,c}[i]=-1]} \\ &= \lambda_1[b_{j,c,l}[i]] + \lambda_2^p[b_{j,c}[i]], \\ &j = 1, \ldots, KN_U, \ c = 1, \ldots, C, \ l = 1, \ldots, L,\end{aligned} \tag{22}$$

where C is the number of bits used to map the constellation, $\lambda_2^p[b_{j,c}[i]] = \log\frac{P[b_{j,c}[i]=+1]}{P[b_{j,c}[i]=-1]}$ is the *a priori* LLR of the code bit $b_{j,c}[i]$, which is computed by the MAP decoder processing the jth data stream in the previous iteration, interleaved and then fed back to the WL-MB-DF detector. The superscript ^{p} denotes the quantity obtained in the previous iteration. Assuming equally likely bits, we have $\lambda_2^p[b_{j,c}[i]] = 0$ in the first iteration for all streams. The quantity $\lambda_1[b_{j,c,l}[i]] = \log\frac{P[\boldsymbol{r}_a[i]|b_{j,c,l}[i]=+1]}{P[\boldsymbol{r}_a[i]|b_{j,c,l}[i]=-1]}$ represents the *extrinsic* information computed by the detector based on the received data $\mathbf{r}_a[i]$, and the prior information about the code bits $\lambda_2^p[b_{j,c}[i]]$, $j = 1, \ldots, KN_U, \ c = 1, \ldots, C$ and the ith data symbol.

For the MAP decoding, we assume that the interference plus noise at the output $\boldsymbol{z}_{j,l}[i]$ of the linear receive filters is Gaussian. Thus, for the jth stream, the lth branch and the qth iteration the soft output of the WL-MB-DF detector is

$$z_{j,l}^{(q)}[i] = V_{j,l}^{(q)} s_{j,l}[i] + \xi_{j,l}^{(q)}[i], \tag{23}$$

where $V_{j,l}^{(q)}[i]$ is a scalar variable equivalent to the magnitude of the channel corresponding to the jth data stream and $\xi_{j,l}^{(q)}[i]$ is a Gaussian random variable with variance $\sigma^2_{\xi_{j,l}^{(q)}}$. Since we have $V_{j,l}^{(q)}[i] = E\big[s_{j,l}^*[i] z_{j,l}^{(q)}[i]\big]$ and $\sigma^2_{\xi_{j,l}^{(q)}}[i] = E\big[|z_{j,l}^{(q)}[i] - V_{j,l}^{(q)}[i] s_{j,l}[i]|^2\big]$, the receiver can obtain the estimates $\hat{V}_{j,l}^{(q)}[i]$ and $\hat{\sigma}^2_{\xi_{j,l}^{(q)}}[i]$ via time averages. These estimates are used to compute the *a posteriori* probabilities $P[b_{j,c,l}[i] = \pm 1 | z_{j,l}^{(q)}[i]]$ which are de-interleaved and used as input to the MAP decoder. In what follows, it is assumed that the MAP decoder generates APPs $P[b_{j,c,l}[i] = \pm 1]$, which are used to compute the input to the feedback filter $\boldsymbol{f}_{j,l}$. From (23) the extrinsic information generated by the iterative WL-MB-DF is given by

$$\lambda_1[b_{j,c,l}[i]] = \log \frac{\sum_{\mathbb{S}\in\mathbb{S}_c^{+1}} \exp\Big(-\frac{|z_{j,l}^{(q)}[i] - V_{j,l}^{(q)}\mathbb{S}|^2}{2\sigma^2_{\xi_{j,l}^{(q)}}[i]}\Big)}{\sum_{\mathbb{S}\in\mathbb{S}_c^{-1}} \exp\Big(-\frac{|z_{j,l}^{(q)}[i] - V_{j,l}^{(q)}\mathbb{S}|^2}{2\sigma^2_{\xi_{j,l}^{(q)}}[i]}\Big)}, \tag{24}$$

where $\mathbb{S}_c^{+1}$ and $\mathbb{S}_c^{-1}$ are the sets of all possible constellations that a symbol can take on such that the cth bit is 1 and -1, respectively. The iterative WL-MB-DF detector chooses the LLR from a list of L candidates for the decoding iteration as

$$\lambda_1[b_{j,c,l_{\text{opt}}}[i]] = \arg\max_{1\leq l\leq L} \lambda_1[b_{j,c,l}[i]], \tag{25}$$

where the selected estimate is the value $\lambda_1[b_{j,c,l_{\text{opt}}}[i]]$ which maximizes the likelihood and corresponds to the most likely bit. Based on the selected prior information $\lambda_1^p[b_{j,c,l_{\text{opt}}}[i]]$ and the trellis structure of the code, the MAP decoder processing the jth data stream and the lth branch computes the *a posteriori* LLR of each coded bit as described by

$$\begin{aligned}\Lambda_2[b_{j,c}[i]] &= \log\frac{P[b_{j,c}[i]=+1|\lambda_1^p[b_{j,c,l_{\text{opt}}}[i]; \text{decoding}]}{P[b_{j,c}[i]=-1|\lambda_1^p[b_{j,c,l_{\text{opt}}}[i]; \text{decoding}]} \\ &= \lambda_2[b_{j,c}[i]] + \lambda_1^p[b_{j,c,l_{\text{opt}}}[i]].\end{aligned} \tag{26}$$

Note that the output of the MAP decoder is the sum of the prior information $\lambda_1^p[b_{j,c,l_{\text{opt}}}[i]]$ and the extrinsic information $\lambda_2[b_{j,c}[i]]$ produced by the MAP decoder. This extrinsic information is the information about the coded bit $b_{j,c}[i]$ obtained from the selected prior information about the other coded bits $\lambda_1^p[b_{j,c,l_{\text{opt}}}[k]]$, $j \neq i$ [21]. The MAP decoder also computes the *a posteriori* LLR of every information bit, which is used to make a decision on the decoded bit at the last iteration. After interleaving, the extrinsic information obtained by the MAP decoder $\lambda_2[b_{j,c}[i]]$ for $j = 1, \ldots KN_U$, $c = 1, \ldots, C$ is fed back to the WL-MB-DF detector, as the prior information about the coded bits of all streams in the subsequent iteration.

V. Simulations

In this section, the bit error ratio (BER) performance of the WL-MB-DF and other relevant MIMO detection schemes is evaluated. The matched-filter, the SIC receivers [11] with linear and WL-MMSE receive filters, the LAS algorithm [9], [10] with linear MMSE receive filters, the MB-MMSE-DF [15] and the proposed WL-MB-DF techniques with error propagation mitigation techniques are considered in the simulations. The channel coefficients are static and obtained from complex Gaussian random variables with zero mean and unit variance. The modulation employed is either QPSK. I/Q imbalance in the RF chains was implemented as a random unequal I/Q imbalance in receiver branches (g_i and ϕ_i were uniformly distributed in $[0.85, 1.15]$ and $[-15^0, 15^0]$, respectively). It is assumed that all parallel receiver branches have their own hardware. Both uncoded and coded systems are considered. For the coded systems and iterative detection and decoding, a non-recursive convolutional code with rate $R = 1/2$, constraint

length 3, generator polynomial $g = [7\ 5]_{\rm oct}$ and 5 decoding iterations is adopted. The numerical results are averaged over 10^6 runs, packets with $Q = 500$ symbols for uncoded systems and $Q = 1000$ coded symbols are employed and the signal-to-noise ratio (SNR) in dB is defined as $\text{SNR} = 10\log_{10}\frac{KN_U\sigma_{s_k}^2}{RC\ \sigma^2}$, where $R < 1$ is the rate of the channel code and C is the number of bits used to represent the constellation.

The uncoded BER performance of the proposed WL-MB-DF detector and existing schemes is considered with $L = 8$ branches and optimized $\beta_{j,l}$. The results shown in Fig. 2 indicate that WL-MB-DF outperforms MB-DF by up to 5dB in terms of required SNR for the same BER performance, which is followed by the WL-SIC, LAS, SIC, and the RMF detectors.

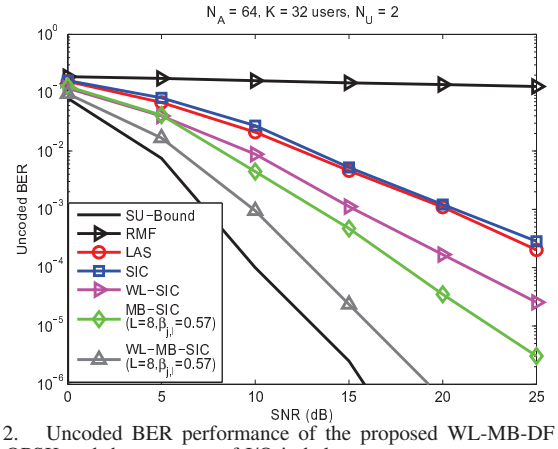

Fig. 2. Uncoded BER performance of the proposed WL-MB-DF detector with QPSK and the presence of I/Q imbalance.

The coded BER performance of the proposed WL-MB-DF detector and existing schemes is then considered with $L = 8$ branches and optimized $\beta_{j,l}$. The results shown in Fig. 3 indicate that the same performance hierarchy is observed and that I/Q imbalance is responsible for a significant performance degradation of the detector with standard linear MMSE filters.

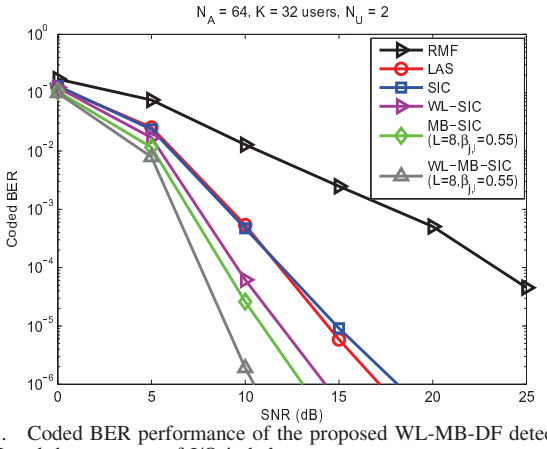

Fig. 3. Coded BER performance of the proposed WL-MB-DF detector with QPSK and the presence of I/Q imbalance.

VI. Conclusions

We have proposed and studied the WL-MB-DF detector for large-scale multiple-antenna systems in the presence of I/Q imbalance. The results have shown that WL-MB-DF can achieve a near-ML performance and mitigate the I/Q imbalance, resulting in significant performance gains over prior art.

References

[1] T. L. Marzetta, "Noncooperative cellular wireless with unlimited numbers of base station antennas," IEEE Trans. Wireless Commun., vol. 9, no. 11, pp. 3590–3600, Nov. 2010.

[2] R. C. de Lamare, "Massive MIMO Systems: Signal Processing Challenges and Future Trends", URSI Radio Science Bulletin, 2013.

[3] R. Aggarwal, C. E. Koksal, and P. Schniter, "On the design of large scale wireless systems", IEEE J. Sel. Areas Commun, vol. 31, no. 2, pp. 215-225, Feb. 2013.

[4] W. Zhang, H. Ren, C. Pan, M. Chen, R. C. de Lamare, B. Du and J. Dai, "Large-Scale Antenna Systems With UL/DL Hardware Mismatch: Achievable Rates Analysis and Calibration", IEEE Trans. Commun., vol.63, no.4, pp. 1216-1229, April 2015.

[5] C. Shepard, H. Yu, N. Anand, L. E. Li, T. L. Marzetta, R. Yang, and L. Zhong, "Argos: Practical many-antenna base stations," in ACM Int. Conf.Mobile Computing and Networking (MobiCom), Istanbul, Turkey, Aug. 2012.

[6] X. Gao, F. Tufvesson, O. Edfors, and F. Rusek, "Measured propagation characteristics for very-large MIMO at 2.6 GHz," in Proc. of the 46th Annual Asilomar Conference on Signals, Systems, and Computers,, Pacific Grove, California, USA, Nov. 2012.

[7] H. Q. Ngo, E. G. Larsson, and T. L. Marzetta, "Energy and spectral efficiency of very large multiuser MIMO systems", IEEE Trans. Commun., vol. 61, no. 4, pp. 1436-1449, Apr. 2013.

[8] H. Yang and T. L. Marzetta, "Performance of conjugate and zero-forcing beamforming in large-scale antenna systems," IEEE J. Sel. Areas Commun., vol. 31, no. 2, pp. 172–179, Feb. 2013.

[9] K. Vardhan, S. Mohammed, A. Chockalingam and B. Rajan, "A low-complexity detector for large MIMO systems and multicarrier CDMA systems", IEEE J. Sel. Commun., vol. 26, no. 3, pp. 473-485, Apr. 2008.

[10] P. Li and R. D. Murch, Multiple Output Selection-LAS Algorithm in Large MIMO Systems, IEEE Commun. Lett., vol. 14, no. 5, pp. 399-401, May 2010.

[11] J. W. Choi, A. C. Singer, J Lee, N. I. Cho, "Improved linear soft-input soft-output detection via soft feedback successive interference cancellation," *IEEE Trans. Commun.*, vol.58, no.3, pp.986-996, March 2010.

[12] P. Li, R. C. de Lamare and R. Fa, "Multiple Feedback Successive Interference Cancellation Detection for Multiuser MIMO Systems," *IEEE Transactions on Wireless Communications*, vol. 10, no. 8, pp. 2434 - 2439, August 2011.

[13] R.C. de Lamare, R. Sampaio-Neto, "Minimum mean-squared error iterative successive parallel arbitrated decision feedback detectors for DS-CDMA systems", IEEE Trans. Commun., vol. 56, no. 5, May 2008, pp. 778-789.

[14] R.C. de Lamare and R. Sampaio-Neto, "Adaptive reduced-rank equalization algorithms based on alternating optimization design techniques for MIMO systems," IEEE Trans. Veh. Technol., vol. 60, no. 6, pp. 2482-2494, July 2011.

[15] R. C. de Lamare, "Adaptive and Iterative Multi-Branch MMSE Decision Feedback Detection Algorithms for Multi-Antenna Systems", *IEEE Trans. Wireless Commun.*, vol. 14, no. 10, October 2013.

[16] T. Schenk, *RF Imperfections in High-rate Wireless Systems: Impact and Digital Compensation*, 1st ed. Springer, Feb. 2008.

[17] S. Buzzi, M. Lops, and S. Sardellitti, "Widely linear reception strategies for layered space-time wireless communications", IEEE Trans. Sig. Proc., vol. 54, no. 6, pp. 2252-2262, Jun. 2006.

[18] P. Chevalier and A. Blin, "Widely linear MVDR beamformers for the reception of an unknown signal corrupted by noncircular interferences", IEEE Trans. Sig. Proc., vol. 55, no. 11, pp. 5323–5336, Nov. 2007.

[19] P. Chevalier and F. Dupuy, "Widely Linear Alamouti Receiver for the Reception of Real-Valued Constellations Corrupted by Interferences—The Alamouti-SAIC/MAIC Concept", IEEE Trans. Sig. Proc., Vol. 59, No. 7, July 2011.

[20] A. Hakkarainen, J. Werner, K. R. Dandekar and M. Valkama, "Widely-linear beamforming and RF impairment suppression in massive antenna arrays," Journal of Communications and Networks, vol.15, no.4, pp.383,397, Aug. 2013.

[21] X. Wang and H. V. Poor, "Iterative (turbo) soft interference cancellation and decoding for coded CDMA," *IEEE Trans. Commun.*, vol. 47, pp. 1046–1061, July 1999.